

Thermally stimulated depolarization phenomena in LiF:Ca²⁺ crystals

A. N. Papathanssiou, J. Grammatikakis, and N. G. Bogris

Department of Physics, Section of Solid State Physics, University of Athens, Panepistimiopolis, GR 157 84 Zografos, Athens, Greece

(Received 24 May 1993)

The thermally-stimulated-depolarization-current method is used in order to characterize the dielectric relaxation processes in LiF crystals doped with Ca²⁺ impurities. Results on as-grown samples indicate a space charge and/or an interfacial polarization phenomenon. Thermal perturbation is employed to release free impurity-cation vacancy dipoles. The subsequent bands are critically visualized and one of them is attributed to jumps of the bound-cation vacancy via nearest-neighbor paths.

I. INTRODUCTION

A divalent cation is incorporated into an alkali halide crystal by substituting a host cation, and the excess positive electric charge of the crystal is compensated for by the creation of a cation vacancy with negative effective electric charge. The coexistence of the divalent impurity and the cation vacancy preserves the electrical neutrality of the whole crystal. At low temperatures the number of vacancies is small, due to thermodynamical reasons, so the majority of point defects is created by doping the host crystal with foreign ions.

The mutual electrostatic attraction of the impurity ion and the cation vacancy leads to the formation of an impurity-vacancy (IV) dipole. The vacancy bound to the impurity is positioned at nearest-neighbor (NN) or next-nearest-neighbor (NNN) lattice sites in relation to the lattice site occupied by the impurity. The stabilities of the NN and NNN IV dipole populations are related to the host crystal structure and also to the dopant size. In alkali halide crystals the NN dipoles establish the major defect population; NNN dipoles may exist for impurities with smaller ionic radius than that of the lithium ion.¹ The orientation of an IV dipole corresponds to certain migration processes of the bound-cation vacancy around the impurity that is assumed to occupy a fixed position, although, for dopants with small ionic radii, the interchange of the impurity with the bound-cation vacancy is also possible. The rotational motion of the IV dipoles can be excited by the application of an external dc or ac electric field. Thus dielectric relaxation studies provide information about the dynamics of the IV dipoles. Two parameters are evaluated from such experiments: the activation energy E , which is identical to the migration enthalpy h^m , and the preexponential factor τ_0 of the usual Arrhenius relation that is directly correlated with the migration entropy of the jumping procedure. The first characterizes the immediate surrounding of the moving defect, while the latter characterizes the whole nonperfect lattice, i.e., the matrix together with the defects.

The migration process of the bound vacancies in lightly doped ionic crystals with NaCl structure is governed by the host material itself, and, on the other hand, by the size of the impurity. Therefore, the impurity is used as a probe sensitive to electrostatic and elastic contributions

to the migration process. Heavy doping of the crystal induces additional electrostatic and elastic contributions since the immediate environment of the migrating species and their frequency spectrum change strongly. There is experimental evidence that these phenomena, which dominate especially in alkaline-earth fluorides, are negligible in alkali halide crystals.² In alkali halide crystals with closed-shell alkaline-earth dopants, with the exception of lithium fluoride, the experimentally evaluated energy needed for the reorientation of NN defect dipoles was found to increase on increasing the ionic radius of the impurity, and this aspect was theoretically justified.³ In lithium fluoride the situation is the opposite: a decrease in the activation energy is observed,⁴⁻¹⁵ while to the best of our knowledge, only one model¹⁰ considering certain migration paths and assuming a lattice distortion around the dipole explains the experimental data provided by different researchers. The results of the present work on lithium fluoride with calcium impurities (where no dielectric relaxation data exist), together with some previously published works of ours,¹¹⁻¹⁵ clarifies the situation for impurities larger than that of lithium.

The Gibbs free energy of an alkali halide crystal is minimized by the contribution of the IV dipoles to the formation of clusters with certain configurations, or of some larger aggregates. Any kind of formation with nonzero dipolar moment can be visualized as a single dipole. Doping, even below the solubility limit, might lead to the development of new phases: precipitates or vacancy-rich superstructures.^{16,17} Appropriate thermal treatments can remove the system from its equilibrium and change the defect structure destroying certain configurations and releasing free IV dipoles.

In a dielectric, apart from the localized dipolar species, free charges can exist in the bulk. The polarization of a crystal results in the motion of free carriers, and a transition from a random to a nonrandom state occurs (space-charge formation) provided that the mobility of the moving charges is high at the temperature where the field was applied. The migration of these carriers can also be impeded by some obstacle (i.e., a dislocation, or an interface separating high and low conductivity areas) that traps them. The exact mechanisms of such free-carrier phenomena can hardly be understood exactly, and often speculations (in some cases firmly established) are pro-

posed. Finally, the motion of free carriers within highly conductive territories embedded into the matrix can yield to delocalized dipoles, and the subsequent phenomenon is called Maxwell-Wagner-Sillars (MWS) or interfacial polarization. Up to date work on the dielectric properties of alkali halides is mainly visualized from a point-defect viewpoint. Concerning low-temperature space-charge and/or trapping phenomena, one has to distinguish the work of McKeever and Huges,¹⁸ while interfacial polarization phenomena were thoroughly examined mainly by Suszyńska and Capelletti and her co-workers.¹⁹⁻²⁷

II. EXPERIMENT

A. The method

Since alkali halides are good insulators, the origin of their bulk electric properties at low temperatures is the migration of nonelectronic defects. Hence the response of the bulk crystal to the application of an external static electric field is due to the migration of the bound-cation vacancies, provided that they are associated with impurities or larger complexes with a nonzero electric dipole moment. Low-temperature space-charge motion should not be excluded *a priori*.

The thermally-stimulated-depolarization-currents (TSDC) or ionic thermocurrent (ITC) method is a high-resolution technique for electrical characterization of dielectrics.²⁸⁻³¹ It is assumed that the thermally activated rotation of the dipoles is described by the set of parameters E and τ_0 which match each other by means of the usual Arrhenius equation that gives the temperature dependence of the relaxation time τ :

$$\tau = \tau_0 \exp(E/kT), \quad (1)$$

where k is the Boltzmann's constant. According to this method an external static electric field is applied to the dielectric at constant temperature T_p , usually the room temperature (RT), for a period of time t_p much longer than the relaxation time $\tau(T_p)$; i.e., sufficient enough so as to orient the vast majority of the crystal's dipoles. The polarized crystal is cooled down to the liquid-nitrogen temperature (LNT), where the polarizing field is then removed. The crystal remains polarized since the relaxation time $\tau(\text{LNT})$ of the dipoles is then practically infinite. We short circuit the sample with a sensitive electrometer and raise the temperature, usually at a rate b . Each kind of dipole will be activated at a certain temperature range, liberating a glow-curve-like depolarization current which maximizes at a temperature T_m whenever the condition

$$\frac{d\tau}{dt} = -1 \quad (2)$$

is fulfilled.³² If the crystal is heated at constant heating rate b , this general condition leads to

$$T_m^2 = \frac{bE\tau_0}{k} \exp(E/kT). \quad (3)$$

The equation giving the depolarization current for a

linear heating rate b is the following:

$$i(T) = \frac{AP_0}{\tau_0} \exp(-E/kT) \exp \left\{ \frac{1}{b\tau_0} \int_{T_0}^T e^{-E/kT'} dT' \right\}, \quad (4)$$

where A is the surface area of the sample, and P_0 is the initial polarization.

For $E > kT$, Eq. (4) can be approximated³³ by the analytical form

$$i(T) = i_m \exp \left\{ 1 + \frac{E}{k} \left[\frac{1}{T_m} - \frac{1}{T} \right] - \frac{T^2}{T_m^2} \exp \left[\frac{E}{k} \left[\frac{1}{T_m} - \frac{1}{T} \right] \right] \right\}, \quad (5)$$

where i_m is the peak amplitude.

For a single curve, the relaxation time $\tau(T)$ is provided according to the so-called area method, for the formula

$$\tau(T) = \frac{\int_T^{T_F} i(T) dT}{bi(T)}, \quad (6)$$

where T_F is the temperature at which the current decreases to zero, so an Arrhenius plot (i.e., $\ln \tau$ vs T^{-1}) permits the evaluation of E and τ_0 .

The initial rise part for temperatures up to about $0.1 T_m$ is approximated by

$$i(T) = \frac{AP_0}{\tau_0} \exp(-E/kT) \quad (7)$$

and therefore a logarithmic plot of the current vs T^{-1} directly gives the activation energy E .

A single TSDC peak permits the evaluation of activation energy E and preexponential factor τ_0 for the reorientation process with high accuracy. In ionic crystals these quantities are attributed to a certain jump process, although this is probably an approximation since different jump frequencies might mix together.³⁴ The method provides no information about the symmetry of the dipolar center, so no conjugation can be made directly between the peak and specific relaxation mechanism. On the other hand, in most crystals the existence of a single peak is unrealistic. Usually, many overlapping peaks may appear, therefore several cleaning procedures involving polarization temperature T_p , polarizing field intensity E_p , and poling time t_p are employed. The most well known of them, such as the peak cleaning, partial heating, and thermal sampling techniques, provide the energy spectra. A short description of each method will accompany the experimental results.

B. Experimental details

Lithium fluoride single crystals with a 10^{-2} atomic fraction calcium as an added dopant in the melt, developed in Utah's Crystal Growth Laboratories, were used. In lithium fluoride it is difficult to introduce large impurities, so we performed atomic absorption analyses

that indicated the presence of less than 2000-ppm Ca^{2+} . In the present system the solubility limit is attained at a few tenths ppm,³⁵ therefore we may conclude that most of the impurities were in precipitated phases, an aspect that is certified from our ITC measurements. Samples 1–1.5 mm thick were prepared, and care was taken to avoid contamination from the moisture.

The samples were placed onto platinum electrodes of a cryostat operating from liquid-nitrogen temperature (LNT) up to 400 K. A vacuum better than 10^{-3} Torr was created by appropriate vacuum pumps. The crystals were polarized by using a Keithley 700-A dc power supplier. The temperature was measured by means of a thermocouple fed into the upper electrode that was connected to an Air-Products temperature controller. The temperature rise was monitored by the controller, and the desired (constant) heating rate was attained throughout each TSDC scan. The depolarization current was measured with a Cary 401 electrometer. Current intensities of the order of 10^{-16} A could be detected. The signals from the controller and the electrometer were digitized via an A/D card installed into a personal computer. The data were computer analyzed afterwards.

III. RESULTS AND DISCUSSION

A. As-grown samples

Ionic thermocurrent measurements on as-grown crystals were performed in the temperature range from LNT up to RT. This temperature limitation is necessary because the thermal prehistory of the sample should be strictly controlled; i.e., thermal cycles must have well-defined limits. In some crystals the thermal depolarization current was measured up to 380 K in order to provide an idea about the existence of relaxation mechanisms at temperatures higher than RT. Although these crystals did not exhibit spectra different from the others, we preferred to keep the temperature of the samples below RT. The polarizing external electric-field intensity was usually less than 30 kV/cm, while the heating rate was kept constant and equal to 6 K/min or less.

A typical thermogram on an as-grown crystal is shown in Fig. 1. The current maximizes at about 227 K and close to RT (hereafter called the *A* band and HT band, respectively). The latter is obviously, complex, as a knee appears at about 270 K. Our interest is mainly focused on the *A* band, as it is in the region where the liberated IV dipoles are activated after a thermal treatment.^{5–11,13,14} This study is critical to the interpretation of the experimental results, especially for bands appearing after a quenching: The characterization of the mechanism creating the *A* band will strongly support the attribution of the peak(s) observed after quenching to the rotation of IV dipoles.

1. Study of the *A* band

Concerning the *A* peak, the maximum current intensity I_m together with the total charge Q released (with some uncertainty due to the overlap with the HT band)

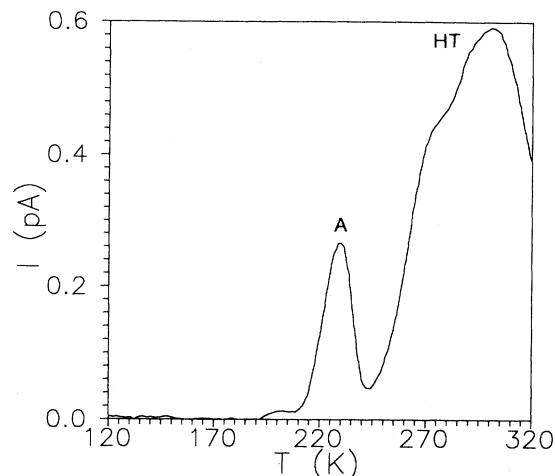


FIG. 1. Thermally stimulated depolarization current emitted from an as-grown sample polarized at 300 K for 6 min under the application of an external field intensity 14.7 kV/cm.

are shown in Fig. 2 as a function of different polarizing field intensities E_p . The supralinear dependence gives some slight evidence that the peak probably does not originate from a dipolar center. It is important to point out that any information about the field dependence should be viewed critically and may not be used as a firm criterion about the origin (dipolar or space charge) of the peak. A dipolar dispersion results in a linear dependence of the peak amplitude upon the field, but the opposite is not necessarily valid.

The *A*-peak amplitude decreased as the sample thickness was gradually reduced while the polarizing field intensity was kept the same. This verifies that the corresponding phenomenon is not one of volume. Additionally, the same peak was observed on silver-painted crystals and, therefore, any contact phenomenon should be excluded.

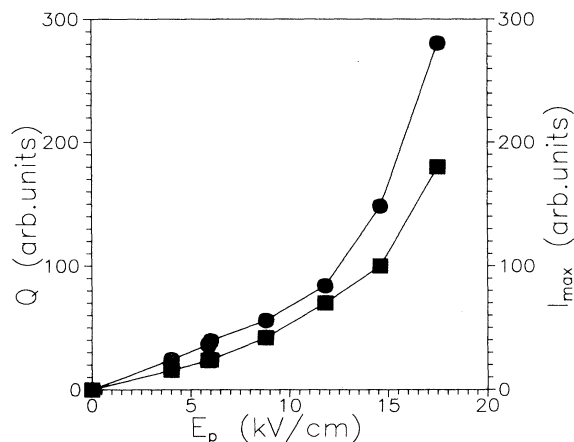


FIG. 2. The field dependence of the charge Q released (squares) and the amplitude I_m (points) for the *A* band.

The shape of the peak is rather symmetrical, indicating either that more than one band strongly overlaps, or that the equations describing the single peak are not of the usual form [i.e., for a space-charge peak it is a crude approximation to accept that it follows Eq. (4)]. In order to achieve efficient cleaning of the peak, we combined the partial depolarization method with the proper selection of the polarizing electric field. The crystal was polarized at RT for 5 min at such an electric-field value which did not cause an overlap of the HT with the *A* peak. We performed a TSDC scan up to about the maximum of the *A* peak, and cooled the crystal down to the LNT. The low-temperature part was therefore partially depolarized, and a subsequent scan revealed what was left from the peak. In Fig. 3 we see that we cannot obtain the peak described in the first-order kinetics equation. A better cleaning of the peak accomplished by partially depolarizing the peak twice or more did not alter the symmetrized shape of the remaining peak. The energy spectra of this mechanism was evaluated by applying the partial heating technique. The sample was polarized once at RT, and the TSDC scan was interrupted as soon as we obtained an initial rise current, by immediately freezing the sample at a temperature T_c . This procedure was repeated many times until we reached RT by depolarizing the relaxation mechanisms step by step. A logarithmic plot of the current versus the inverse temperature provides a linear part *a* with slope equal to $-E/k$ according to Eq. (7). This experimental method (in the sense of successively slicing the TSDC spectra) is not very common in the study of ionic crystals, probably due to the fact that the ionic thermo-current is generally low enough in comparison to that emitted from different kinds of dielectrics such as polymers. In Fig. 4 the activation energies versus the temperature T_c , where the sample was frozen are displayed. We conclude that for the *A* peak ($210 < T_c < 240$ K) we have a distribution around 0.8 eV. Notice that this value is close to the migration enthalpy of the free-cation vacancy.^{12,15} On the other hand, by using Eq. (3) we may have

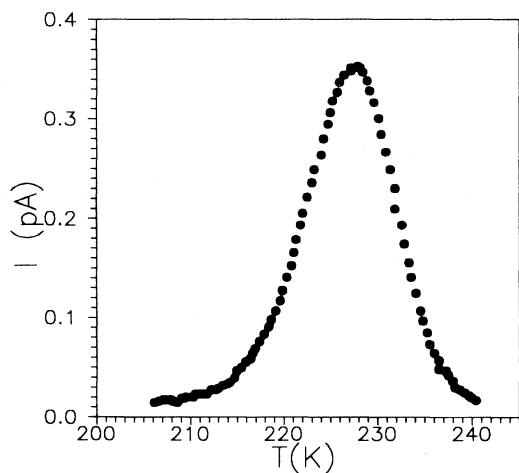


FIG. 3. The cleaned *A* band. Proper selection of the polarizing conditions prevented overlap with the HT band. The mechanism was previously depolarized up to its maximum.

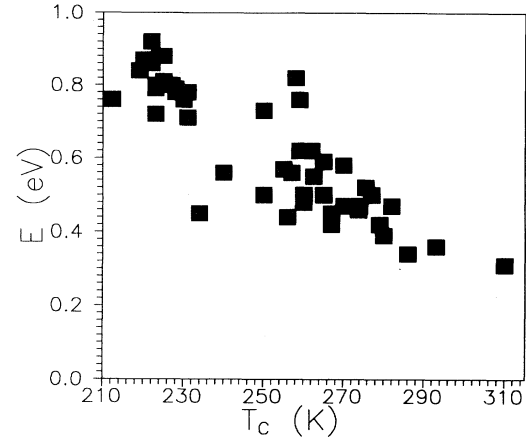


FIG. 4. The energy spectrum obtained with the partial heating method from an as-grown crystal.

a rough estimate of τ_0 , which is found to be around 10^{-16} sec.

Polarization at lower temperatures (but always higher than the maximum T_m) did not produce any significant variation of the temperature T_m where the current maximizes [Fig. 5(a)]. The amplitude of the band gradually decreased on decreasing T_p for the same polarization field intensity and polarization time. Reaching T_m we observed that this temperature acts as a lower polarization limit even for long polarization intervals; i.e., we could not reach any detectable polarization state when $T_p < T_m$ even for long polarization times (about 30 min). We notice that the time needed to orient the polarizable entities, calculated by replacing a mean value of E and τ_0 in the Arrhenius equation, was no more than a couple of minutes. Whatever the uncertainty in determining the relaxation time, we speculate that in this temperature region any kind of localized dipolar center of the usual

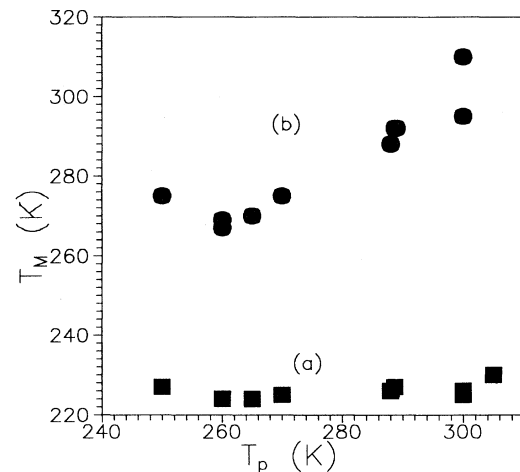


FIG. 5. The variation of the temperature T_m where the current maximizes vs different polarization temperatures T_p (a) For the *A* peak. (b) For the complex HT band.

form should be oriented.

A careful view in Fig. 6 shows that there is a slight dependence of T_m on the intensity of the external electric field E_p , keeping constant T_p and t_p . Keeping in mind that the heating rate was the same in all these scans, and that therefore the aspect of a low reproducibility is definitely excluded, we conclude that this is a feature of the relaxation process itself. There is a report³⁶ on such field-dependent phenomena concerning the migration of free carriers.

The use of insulating electrodes, such as two thin teflon foils placed between the sample and the metal electrodes [the metal-insulator-sample-insulator-metal (MISIM) structure], is expected to produce a shift in the maximum temperature T_m of a space charge ITC peak.³⁷ In the present case, we applied the usual external polarizing field in a MISIM configuration, but no significant shift was observed, indicating a dipolar (or, dipolarlike) origin. We used only 0.1-mm-thick good-quality teflon in both MISIM and MISM (metal-insulator-sample-metal) structures, but we did not try thicker insulating foil since this might cause temperature differences between the metal electrodes and the sample.

Attribution of the A band to a space-charge phenomenon is based on the experimental results that were arranged above: The inadequacy for polarizing at $T_p < T_m$, the supralinearity of the peak amplitude upon the field, the dependence of T_m vs E_p , and the symmetrical shape of the curve. The only opposing point is the dipolar feature exhibited when we use teflon electrodes. The temperature region where the A -band relaxation mechanism is activated is rather low (a few tens of degrees below RT). In general, a space charge involves the motion of the charge carriers at distances longer than the interatomic spacing, and consequently such a conduction mechanism is expected to provide a TSDC peak maximized at relatively high temperatures. But a low-temperature space charge is quite acceptable, according to a paper of McKeever and Huges¹⁸ concerning a low-

temperature space charge in alkali halide crystals.

Our results can also be explained by means of the interfacial polarization theory that applies in inhomogeneous dielectrics. With the assumption that inclusions of highly conducting material fed into a host material with lower conductivity exist (in other words, boundaries separating different constituents of the crystal), one can find physical arguments for additional low-frequency Debye dielectric loss (apart from the contribution of each component itself).³⁸ Following different approximations one may derive analytical expressions for the complex dielectric constant, and a relaxation time corresponding to the aforementioned response. A thermally activated relaxation time results in the appearance of a peak in a TSDC spectra.

In alkali halides certain TSDC peaks were attributed by Capelletti and co-workers¹⁹⁻²⁷ to MWS polarization phenomena originating either from vacancy-rich Suzuki superstructures or from the highly conductive territories surrounding the dislocations. These peaks are maximized at temperatures higher than RT. In rare-earth-doped alkaline-earth fluorides Suarez *et al.*³⁹ report a MWS peak which, for a certain impurity concentration range, is located at considerably lower temperatures which are comparable to the maximum temperature of our A -band.

Specific features of the crystals we used strongly support the last idea. The inadequacy of dissolving the added impurity quantity in the solid solution and, therefore, the presence of strong precipitation, motivates the development of a dihalide-precipitated phase¹ and/or a highly conductive⁴⁰ local superstructure, namely the Suzuki phase.¹ These vacancy-rich territories are possible areas where a diffusion process can occur, especially the inability to polarize the A peak below its maximum, justifying a spacelike motion. This agrees with the space-charge features of the A peak, and the activation energy of 0.8 eV we evaluated experimentally probably indicates the motion of free vacancies since this value is close to the free-cation vacancy migration enthalpy. Dipolar characteristics can be stimulated by multiple relations of cation vacancies bound to different neighbor calcium cations,²⁵ and from MWS relaxation developing at the boundaries of the phase. For the case in which a TSDC peak originates from a MWS phenomenon (usually treated as a dipolar band), there is no reason to have the usual glow curve peak shape. We see that the existence of a superstructure in the host material gives rise to different and probably correlated phenomena (e.g., the diffusion process within a closed area with the resulting interfacial polarization).

2. Study of the HT band

The HT band arises from at least two mechanisms. One of them is present as a knee at 270 K (Fig. 1). Our experiments show that this complex band is not sensitive to the material of the electrodes, and so this temperature region for the present system is not a serious candidate for the appearance of injection or space charge phenomena. In Fig. 5(b), the dependence of the temperature T_m , where the current of the dominant mechanism maximizes

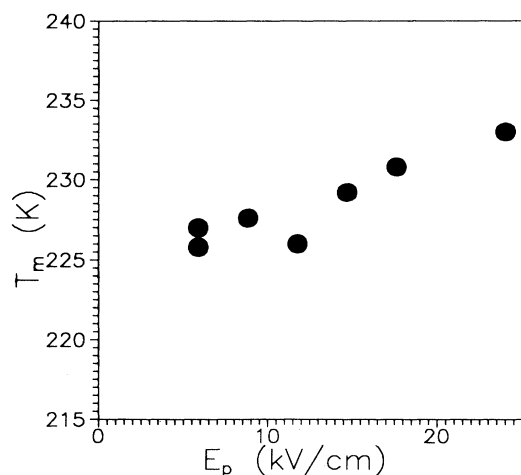


FIG. 6. The dependence of the temperature T_m , upon the intensity E_p of the external polarizing field, where the A peak maximizes.

in relation to the polarization temperature T_p , shows that rotation of some complexes takes place at a nonzero dipolar moment with distribution in the relaxation time. This distribution can affect the activation energy in the sense of some mutually interacting cluster formations or/and the preexponential factor τ_0 as a quantity sensitive to frequency spectrum changes. In Fig. 4 we may have an estimate of the activation energies obtained by slicing the TSDC spectra with the partial heating method. For reasons explained at the beginning of this section concerning the thermal prehistory of the samples, we were limited within RT. We notice that the energies found are low. One expects that at high temperature the thermal energy should activate dipolar centers which correspond to higher activation energies, although our values are in agreement with extensive results for the high-temperature region.⁴¹ Recent research on alkali halides¹⁹⁻²⁷ attributes these bands to MWS phenomena due to the existence of the Suzuki phase or to the role of line defects. Thermal perturbation changes but does not eliminate these contributions, although Raman spectroscopy indicates the annihilation of the Suzuki phase,²⁵ leading to the speculation that cluster and/or Suzuki phase precursor aggregates play a significant role. This is exactly what we support, because our HT bands are strongly affected by the quenching procedure: all of the HT band may be destroyed, or at least the spectra in this range may be clarified. We observe that this phenomenon depends on the speed of the quench, and is related to the problems of the quenching process itself (see also Sec. II).

B. Thermally treated samples

In the present section we shall deal with the bands that appear after quenching the crystals. With the aim of liberating free IV dipoles from any cluster formation, we thermally perturb and afterward freeze the crystals. In such procedure we are trying to produce as many IV dipoles as possible, and to maximize the size of the subsequent TSDC peak. In order to find the best combinations of annealing temperature and annealing time that liberates as many IV dipoles as possible, we tried temperatures ranging from 400 to 600 °C for periods from 10 min to 8 h. The proper selection of annealing temperature and time fulfills two purposes: First, from the area of the (maximized) IV dipole TSDC peak, we may evaluate the population of IV dipoles existing in the matrix. Second, we certify that the peak obtained is stimulated by the re-orientation of free IV dipoles and not by an aggregate, as a result of an aging procedure that might have occurred during the annealing.

The stage that follows the annealing is the rapid decrease of the crystal's temperature, usually at RT. This will freeze the released dipole population unless the freezing rate is low. The annealed crystals are quickly cooled by placing them onto a copper block, or by dropping them into acetone or liquid nitrogen to avoid the aggregation of the IV dipoles. The first way is the usual one, but it has the disadvantage that the sample (which is also a good heat insulator) is cooled inhomogeneously.⁹ The

second method is the best one but is often destructive of the samples, which oftentimes crack. In this case it is quite probable that internal stress fields develop into the sample and affect the rotation of the IV dipoles (which act as electric and elastic dipoles as well).

In Fig. 7(a) we present a TSDC thermogram of an annealed and quenched crystal. By comparison with the spectra recorded on a virgin sample (Fig. 1) we see that the HT is sensitive to thermal treatments, with the simultaneous appearance of a new low-temperature band hereafter called the LT band. In the present section we emphasize the LT peak. This complex band obtained from two different experiments on quenched samples is depicted in Fig. 7(b). The polarization conditions are presented in the figure caption. By performing different cleaning procedures we found that this complex band consists of three strongly overlapping peaks with maxima at 189,

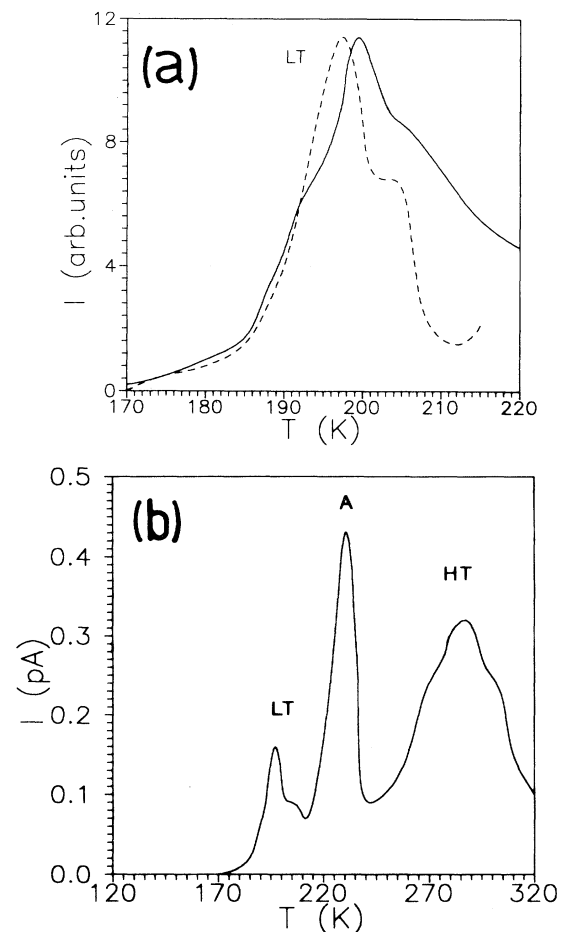


FIG. 7. TSDC thermograms of crystals that have undergone an annealing and quenching procedure. (a) From a sample that was polarized at RT. (b) The LT band, which appears after the quenching. Dashed line: Annealed at 873 K for 1.55 h, and quenched to RT by placing the sample onto a copper block. Solid line: Annealed at 873 K for 2 h, and quenched to RT by dropping the sample into dry acetone. The samples were polarized with $E_p = 17$ kV/cm for 4–5 min at RT. Different heating rates were used to exhibit each mechanism.

197, and 206 K, respectively. A logarithmic plot of the initial rise current vs T^{-1} , according to the method expressed through Eq. (7), gives an estimate of the energy $E=0.6$ eV for the 189-K peak. Although this estimate is crude, due to the strong overlap, it provides evidence of the energy of the first band. Evaluation of the energy parameters (E and τ_0) of each relaxation mechanism requires isolation of each of the peaks.

The first peak (Fig. 8) maximizing at 189 K was isolated by applying the peak cleaning method; i.e., by performing the usual experimental procedure described in Sec. II A with the proper selection of polarization temperature and polarization time that will orient only the dipoles we desire. Figure 8 comes from a sample polarized at 184 K for 5 min which had previously been annealed at 873 K for 45 min and quenched to RT. The area method permits the calculation of the relaxation time at each temperature via Eq. (6). A linear relation of $\ln\tau$ vs T^{-1} (Fig. 9) certifies the good cleaning, and that the simple TSDC equation well describes the glow-curve-like peak. The energy parameters are included in Table I. The results are highly reproducible. The maximum of the peak does not shift when we use teflon electrodes, while E and τ_0 remain the same.

The second peak with a maximum at 197 K is located between the two others (189 and 206 K). For its isolation the method we successfully used is a kind of thermal sampling. In the usual thermal sampling method, sometimes called fractional polarization,³⁰ we polarize at a temperature window as we cool the sample, while the subsequent temperature raise is expected to stimulate a TSDC peak in the window. An equivalent method⁴² that polarizes the desired dipolar species with simultaneous elimination of undesirable neighboring mechanisms is to polarize at a given temperature T_s (in the present case at the temperature where the current maximizes) for a period of time t_p and, by keeping the temperature T_s constant, depolarize for a period t_d . Immediately afterward the crystal is frozen and a TSDC scan follows, giving rise to the relaxa-

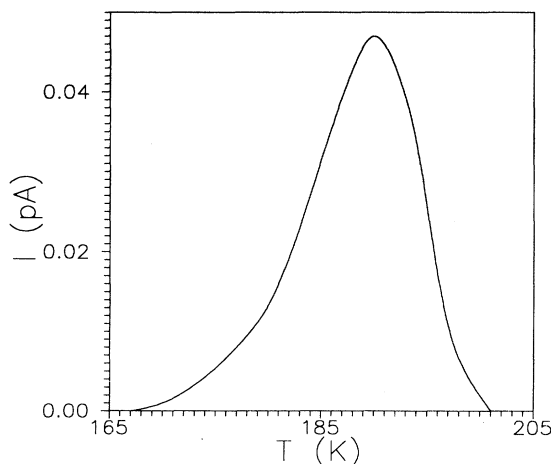


FIG. 8. The first mechanism (189 K) involved in the band depicted in Fig. 7. For reasons explained in the text this band is attributed to the rotation of IV dipoles.

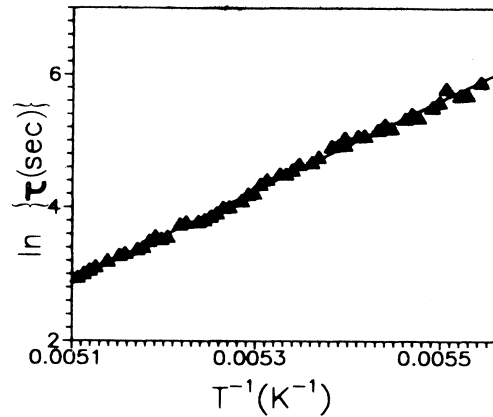


FIG. 9. The Arrhenius plot of the peak with maximum at 189 K that is drawn in Fig. 8. The linearity certifies the efficient cleaning, permitting an accurate determination of E and τ_0 .

tion mechanism dominating at the temperature region around T_s , provided that we have made a proper selection of t_p and t_d . This method provided single peaks that fit well to the TSDC equation. For the same mechanism we also successfully applied the usual peak cleaning method, which again gave a single peak obeying Eq. (4). In Fig. 10 we demonstrate the result of the peak cleaning and thermal sampling methods in order to provide an idea of the efficiency of the first technique. In the first method we polarized at 187 K for 4.5 min. In the latter, we polarized at 198-K for 2 min, depolarized at the same temperature, and immediately after cooled down to LNT.

For the third band located at 206 K it proved difficult to fully isolate the TSDC band. When the quenched crystal was polarized at RT, the peak strongly interfered with the A band referred in Sec. II. A peak cleaning procedure at lower temperatures ($T_p=190$ K, $t_p=3$ min) combined with successive partial depolarizations up to about 199 K was not quite adequate, since the remaining cleaned peak showed a long high-temperature tail. Therefore the energy parameters were estimated with the initial rise method and, more accurately, by performing a fit to the maximum current I_m and maximum temperature T_m as input parameters according to Eq. (5). By means of this fit we may avoid the high-temperature range (above T_m) where some overlap exists, while the experimental points used in the fitting are adequate enough.

The area of the complex peak is maximized for a certain annealing temperature and duration, while longer annealing results in a gradual decrease, a phenomenon

TABLE I. Energy parameters of the overlapping low-temperature mechanisms that appear after quenching the crystals and constitute the LT band.

T_m (K)	E (eV)	τ_0 (sec)
189	0.59	1.66×10^{-14}
197	0.98	1.39×10^{-24}
206	0.99	2.22×10^{-23}

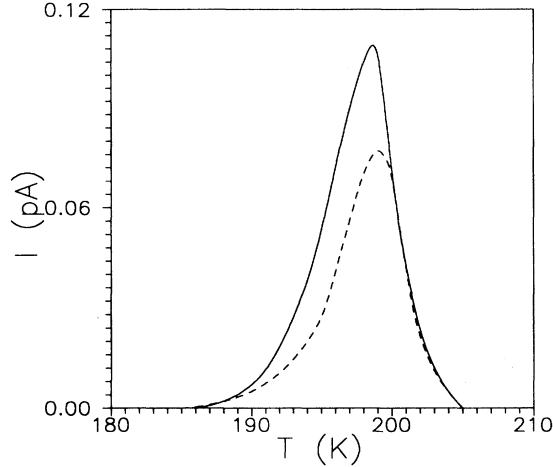


FIG. 10. Dashed line: The result of the usual peak cleaning procedure. Solid line: A modification of the thermal sampling technique. The details are presented in the text.

that certifies that some IV dipoles are liberated, that for longer annealing times aging (and probably some clustering) occurs. The above bands appear in the temperature region where free IV dipoles can be activated. We believe that the 189-K peak is related to jumps of the bound-cation vacancy from NN to NN lattice sites, because the activation energy of the first band is very close to these reported for the NN jumps in LiF doped with other divalent impurities, while the inverse of the preexponential factor is quite reasonable in comparison to the frequency of the transverse-optic mode of the LiF atomic chain. This attribution is strongly supported by preliminary measurements of the imaginary part of the dielectric constant performed in the frequency domain,⁴³ which reveal a relaxation mechanism with $E=0.58$ eV and $\tau_0 \approx 10^{-11}$ sec. On the other hand, assuming that NN dipoles are responsible for the 189-K peak, the area enclosed under this peak permits us to estimate the amount of these dipoles, which is found to be much less than 100 ppm. This result is consistent with information presented in Sec. II B.

Accepting that attribution of the 189-K peak to the jumps of the bound-cation vacancy through NN paths is physically well established, we may proceed to the evaluation of the vibrating frequency of the real lattice (i.e., including defects). We use the so-called $cB\Omega$ model that interconnects the point-defect parameters for a formation, migration, or activation process with the bulk properties of the host material. The $cB\Omega$ model states that the ratio s^i/h^i , where s^i and h^i denote the entropy and the enthalpy, while $i=f, m, a$ corresponds to a formation, migration, or activation process, is equal to the bulk property

$$F = \frac{-\beta B + [\partial B / \partial T]_p}{B - T\beta B - T[\partial B / \partial T]_p}, \quad (8)$$

where β is the thermal expansion coefficient, and B the bulk modulus of the host crystal. For LiF it was found⁴⁴

that $F \approx 3 \times 10^{-4} \text{ K}^{-1}$. ITC experiments can also lead to the evaluation of the ratio s^m/h^m corresponding to the bound-cation vacancy motion. The activation energy E is identical to h^m , while the migration entropy s^m for NN \rightarrow NN jumps is given by the formula⁴⁴

$$s^m = k \ln \frac{1}{2\nu\tau_0}, \quad (9)$$

where ν is the vibration frequency of the migrating defect. By rewriting Eqs. (8) and (9), we obtain

$$k \ln \left[\frac{1}{2\nu\tau_0} \right] = Fh^m. \quad (10)$$

By replacing h^m and τ_0 by the values found for the 189-K peak (Table I), we obtain $\nu = 4.18 \times 10^{13} \text{ sec}^{-1}$. It is worth noticing that⁴⁴ $\nu_{\text{TO}}(k \rightarrow 0) = 0.92 \times 10^{13} \text{ sec}^{-1}$, where ν_{TO} corresponds to the long-wavelength transverse-optical mode.

The two high-energy peaks (197 and 206 K) are difficult to correlate with some known jump paths followed by the migrating bound-cation vacancy. Additionally, prefactors τ_0 are extremely low. Annealing at 873 K for about 1 h and subsequent quenching is enough to liberate most of the IV dipoles (189-K peak). If the crystal is annealed at the same temperature for about 2 h the high-energy peaks also maximize, but not at the expense of the 189-K peak, indicating that the high-energy peaks are not due to the aggregation of simple IV dipoles. It is worth noting from our LiF crystals doped with alkaline-earth cations that a high-energy band adjoining the IV peak was observed only in LiF:Ba²⁺.¹⁴ Hence we may state that the appearance of these high-energy bands might be related to the large impurity size.

IV. CONCLUSIONS

In the present study we have made an electrical characterization of as-grown LiF:Ca²⁺ crystals by the sensitive TSDC method. We have detected two bands, namely

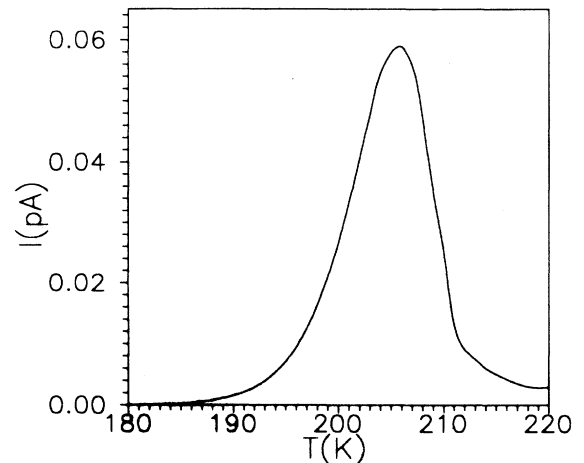


FIG. 11. The third peak participating to the LT band (Fig. 7). Its maximum is located at 206 K.

A and HT. The HT complex peak presents the properties of the peaks detected in alkali halides by different authors. We proved that the *A* band, appearing in the region where IV dipoles are usually activated in LiF doped with a variety of divalent impurities, is not related to a simple rotation of any dipolar species. It is either related to a low-temperature space charge or to an interfacial polarization involving a diffusion process.

The dynamical properties of dipolar centers released after annealing and subsequent quenching are also presented. Certain criteria indicate that the 189-K peak is stimulated as the cation vacancy bound to the impurity jumps via NN paths. A collection of the recent data reported shows a slow (in comparison to Ref. 5) decrease of

the migration enthalpy of the bound vacancy with the radius of the impurity for impurities larger than the host cation.

ACKNOWLEDGMENTS

We are grateful to Professor P. Varotsos for his suggestions on this work, and to Professor M. Syszyńska (Polish Academy of Sciences, Poland) for the discussions on dislocation related MWS phenomena. We are also indebted to Professor E. Laredo (Universidad Simón Bolívar, Venezuela) for the discussions and the additional information about ITC peaks due to interfacial polarization.

- ¹F. Agullo-Lopez, C. R. A. Catlow, and P. D. Townsend, *Point Defects in Materials* (Academic, London, 1988).
- ²P. Aceituno and F. Cussó, *Phys. Rev. B* **25**, 7577 (1982).
- ³C. R. A. Catlow, J. Corish, J. M. Quigley, and P. W. M. Jacobs, *J. Phys. Chem. Solids* **41**, 231 (1980).
- ⁴R. M. Grant, Jr. and J. R. Cameron, *J. Appl. Phys.* **37**, 3791 (1966).
- ⁵C. Lai and P. Berge, *J. Phys. (Paris)* **28**, 821 (1967).
- ⁶P. R. Moran and D. E. Fields, *J. Appl. Phys.* **45**, 3266 (1974).
- ⁷S. W. S. McKeever and D. M. Huges, *J. Phys. D* **8**, 1520 (1975).
- ⁸S. W. S. McKeever and E. Lilley, *J. Phys. C* **14**, 3547 (1981).
- ⁹S. W. S. McKeever and E. Lilley, *J. Phys. Chem. Solids* **43**, 885 (1982).
- ¹⁰F. Cussó and F. Jaque, *J. Phys. C* **15**, 2875 (1982).
- ¹¹A. B. Vassilikou, J. Grammatikakis, and C. A. Londos, *J. Phys. Chem. Solids* **47**, 727 (1986).
- ¹²J. Grammatikakis, C. A. Londos, V. Katsika, and N. Bogris, *J. Phys. Chem. Solids* **50**, 845 (1989).
- ¹³V. Katsika and J. Grammatikakis, *J. Phys. Chem. Solids* **51**, 1089 (1990).
- ¹⁴V. Katsika, J. Grammatikakis, N. Bogris, A. Kyritsis, and A. Papathanassiou, *Phys. Rev. B* **44**, 12 686 (1991).
- ¹⁵J. Grammatikakis, A. Papathanassiou, N. Bogris, M. Manolopoulos, and V. Katsika, *Phys. Rev. B* **46**, 12 142 (1992).
- ¹⁶D. Figueroa, E. Laredo, and M. Puma, *Solid State Commun.* **25**, 509 (1978).
- ¹⁷A. de Andres and J. M. Calleja, *Solid State Commun.* **48**, 949 (1983).
- ¹⁸S. W. S. McKeever and D. M. Huges, *J. Phys. Chem. Solids* **19**, 211 (1978).
- ¹⁹M. Syszyńska and R. Capelletti, *Cryst. Res. Technol.* **19**, 1385 (1984).
- ²⁰M. Syszyńska and R. Capelletti, *Cryst. Res. Technol.* **19**, 1489 (1984).
- ²¹M. Syszyńska and R. Capelletti, *Cryst. Res. Technol.* **20**, 1363 (1985).
- ²²M. Syszyńska and R. Capelletti, *Acta Phys. Pol. A* **69**, 233 (1986).
- ²³M. Syszyńska and R. Capelletti, *Cryst. Res. Technol.* **23**, 199 (1988).
- ²⁴M. Syszyńska and R. Capelletti, *Acta Phys. Pol. A* **80**, 129 (1991).
- ²⁵G. Benedek, J. M. Calleja, R. Capelletti, and A. Breitschwerdt, *J. Phys. Chem. Solids* **45**, 741 (1984).
- ²⁶R. Capelletti, C. Mora, E. Zecchi, and O. Carranza Torres, *Rad. Eff.* **75**, 93 (1983).
- ²⁷R. Capelletti, L. Foldvari, C. Mora, and S. Prato, *ITC Technique as a Tool to Monitor a New Phase Nucleation in LiF:Ti³⁺ Single Crystals*, 7th International Symposium on Electrets, Berlin, 1991, p. 539.
- ²⁸C. Bucci and R. Fieschi, *Phys. Rev. Lett.* **12**, 16 (1964).
- ²⁹C. Bucci, R. Fieschi, and G. Guidi, *Phys. Rev.* **148**, 816 (1966).
- ³⁰J. Vanderschueren and J. Gasiot, in *Thermally Stimulated Relaxation in Solids*, edited by P. Braunlich (Springer-Verlag, Berlin, 1979), p. 135.
- ³¹J. van Turnhout, in *Electrets*, edited by G. M. Sessler (Springer-Verlag, Berlin, 1980), p. 81.
- ³²P. Varotsos, N. G. Bogris, and A. Kyritsis, *J. Phys. Chem. Solids* **53**, 1007 (1992).
- ³³J. Prakash and A. K. Nishad, *J. Appl. Phys.* **67**, 3468 (1990).
- ³⁴F. Cusso and F. Jaque, *Solid State Commun.* **29**, 283 (1979).
- ³⁵M. C. DeLong (private communication).
- ³⁶T. W. Hickmott, *J. Appl. Phys.* **46**, 2583 (1975).
- ³⁷P. Muller, *Phys. Status Solidi A* **67**, 11 (1981).
- ³⁸L. K. H. van Beek, in *Progress in Dielectrics*, edited by J. B. Birks (Heywood, London, 1967), Vol. 7.
- ³⁹N. Suarez, E. Laredo, F. Lorentzo, A. Bello, and M. Puma, *Solid State Ion.* **38**, 63, (1990).
- ⁴⁰N. Bonanos and E. Lilley, *J. Phys. Chem. Solids* **42**, 943 (1981).
- ⁴¹E. M. Yoshimura and E. Okuno, in *Proceedings of the XII International Conference on Defects in Insulating Materials*, edited by O. Kauert and J. -M. Spaeth (Schloss Nozdkirchen, Germany, 1992).
- ⁴²S. Schröder and H. E. Carius (Ref. 27), p. 581.
- ⁴³A. N. Papathanassiou, J. Grammatikakis, and N. G. Bogris, in *Proceedings of the XII International Conference on Defects in Insulating Materials* (Ref. 41), p. 801. (unpublished).
- ⁴⁴M. Lazaridou, C. Varotsos, K. Alexopoulos, and P. Varotsos, *J. Phys. C* **18**, 3891 (1985).